ISSN 1674-1056
http://cpb.iphy.ac.cn
http://iopscience.iop.org/cpb
中国物理 B
Chinese Physics
中国物理
Chinese Physics B

Analytical studies on the evolution processes of rarefied deuterium plasma shell Z-pinch by PIC and MHD simulations

Cheng Ning(宁成), Xiao-Qiang Zhang(张小强), Yang Zhang(张扬), Shun-Kai Sun(孙顺凯), Chuang Xue(薛创), Zhi-Xing Feng(丰志兴), Bai-Wen Li(李百文)
Citation: Chin. Phys. B . 2018, 27(2): 025207. **doi:** 10.1088/1674-1056/27/2/025207

Journal homepage: http://cpb.iphy.ac.cn; http://iopscience.iop.org/cpb

What follows is a list of articles you may be interested in

Influence of a centered dielectric tube on inductively coupled plasma source: Chamber structures and plasma characteristics

Zhen-Hua Bi(毕振华), Yi Hong(洪义), Guang-Jiu Lei(雷光玖), Shuai Wang(王帅), You-Nian Wang(王友年), Dong-Ping Liu(刘东平)
Chin. Phys. B . 2017, 26(7): 075203. **doi:** 10.1088/1674-1056/26/7/075203

Numerical study on the discharge characteristics and nonlinear behaviors of atmospheric pressure coaxial electrode dielectric barrier discharges

Ding-Zong Zhang(张定宗), Yan-Hui Wang(王艳辉), De-Zhen Wang(王德真)
Chin. Phys. B . 2017, 26(6): 065206. **doi:** 10.1088/1674-1056/26/6/065206

End-on x-ray backlighting experiments for axial diagnostics of wire-array Z-pinch plasma on PPG-1

Shen Zhao(赵屾), Xinlei Zhu(朱鑫磊), Huantong Shi(石桓通), Xiaobing Zou(邹晓兵), Xinxin Wang(王新新)
Chin. Phys. B . 2017, 26(1): 015206. **doi:** 10.1088/1674-1056/26/1/015206

Numerical simulation of a direct current glow discharge in atmospheric pressure helium

Zeng-Qian Yin(尹增谦), Yan Wang(汪岩), Pan-Pan Zhang(张盼盼), Qi Zhang(张琦), Xue-Chen Li(李雪辰)
Chin. Phys. B . 2016, 25(12): 125203. **doi:** 10.1088/1674-1056/25/12/125203

Energy spectrum of multi-radiation of X-rays in a low energy Mather-type plasma focus device

Farzin M. Aghamir, Reza A. Behbahani
Chin. Phys. B . 2014, 23(6): 065203. **doi:** 10.1088/1674-1056/23/6/065203

Analytical studies on the evolution processes of rarefied deuterium plasma shell Z-pinch by PIC and MHD simulations*

Cheng Ning(宁成)†, Xiao-Qiang Zhang(张小强), Yang Zhang(张扬), Shun-Kai Sun(孙顺凯), Chuang Xue(薛创), Zhi-Xing Feng(丰志兴), and Bai-Wen Li(李百文)

Institute of Applied Physics and Computational Mathematics, Beijing 100088, *China*

(Received 25 July 2017; revised manuscript received 16 September 2017; published online 5 January 2018)

In this paper, we analytically explore the magnetic field and mass density evolutions obtained in particle-in-cell (PIC) and magnetohydrodynamics (MHD) simulations of a rarefied deuterium shell Z-pinch and compare those results, and also we study the effects of artificially increased Spitzer resistivity on the magnetic field evolution and Z-pinch dynamic process in the MHD simulation. There are significant differences between the profiles of mass density in the PIC and MHD simulations before 45 ns of the Z-pinch in this study. However, after the shock formation in the PIC simulation, the mass density profile is similar to that in the MHD simulation in the case of using multiplier 2 to modify the Spitzer resistivity. Compared with the magnetic field profiles of the PIC simulation of the shell, the magnetic field diffusion has still not been sufficiently revealed in the MHD simulation even though their convergence ratios become the same by using larger multipliers in the resistivity. The MHD simulation results suggest that the magnetic field diffusion is greatly enhanced by increasing the Spitzer resistivity used, which, however, causes the implosion characteristic to change from shock compression to weak shock, even shockless evolution, and expedites the expansion of the shell. Too large a multiplier is not suggested to be used to modify the resistivity in some Z-pinch applications, such as the Z-pinch driven inertial confinement fusion (ICF) in a dynamic hohlraum. Two-fluid or Hall MHD model, even the PIC/fluid hybrid simulation would be considered as a suitable physical model when there exist the plasma regions with very low density in the simulated domain.

Keywords: shell Z-pinch, PIC and MHD simulations, wire-array Z-pinch

PACS: 52.58.Lq, 52.65.–y, 52.59.Qy **DOI:** 10.1088/1674-1056/27/2/025207

1. Introduction

The Z-pinch of wire-array (liner) has been considered as a promising drive approach to the ignition of inertial confinement fusion (ICF) and its fusion energy application due to its high conversion efficiency from electromagnetic energy stored to kinetic and radiation energy of implosion plasma.[1–6] While its plasma formation and implosion process are very complicated. There are a lot of measured images from the wire-array (without preconditioning) Z-pinch experiments to demonstrate that the majority of wire-array substance has been ablated due to Joule heating and is radially swept inward towards the array axis by $\boldsymbol{j} \times \boldsymbol{B}$ force, while the wire-cores keep stationary at their original positions before its implosion begins.[7–12] So actually inside the wire-array is prefilled with ablated plasma, whose density varies with time and radius. It is possibly very low sometime and somewhere.

In most of simulations of wire-array Z-pinch, the ablation process of wire-array is ignored due to its complexity, and the wire-array is treated as a plasma shell with a precursor plasma inside, or the wires are treated as the metallic gas sources with high density and low temperature.[12,13] The metallic gas is partly ionized and expanded. The ionized gas is driven inward by Lorentz force, and a precursor plasma profile is formed. The density of ablated plasma inside the wire-array is varying all the way, and is possibly very low in the front of the precursor plasma, or the streams of the ablated plasma. For the very low plasma density it should be understood whether the currently used magnetohydrodynamics (MHD) model can accurately describe the magnetic field evolution and the electric fluid movement.

In the practice of Z-pinch simulation, which is mostly based on the radiation magnetohydrodynamics equations (model), for obtaining better simulation results, which agree well with the experimental data, such as convergence ratio, and x-ray power and energy, the electrical resistivity of Z-pinch plasma needs artificially modifing more or less.[12,14] The characteristic results might be obtained through this modification, but the magnetic field evolution and the pinch dynamic process might be changed unexpectedly. It is interesting and important to explore the variations of the magnetic field evolution and the dynamic process with this modification.

The discharged plasma is essentially a system consisting of a large number of charged particles, i.e., electrons and ionized ions. So the Z-pinch plasma can be treated as a huge charged particle system, and can be simulated through

*Projected supported by the National Natural Science Foundation of China (Grant Nos. 11675025, 11135007, and 11405012).

†Corresponding author. E-mail: ning_cheng@iapcm.ac.cn

© 2018 Chinese Physical Society and IOP Publishing Ltd

a particle-in-cell (PIC) code. In principle, it is to solve the Maxwell equations and particle motion equations.[15] Welch *et al.* first realized the fully kinetic particle-in-cell simulation of deuterium gas-puff Z-pinch on a Z machine.[16–18] They made use of the implicit, fully electromagnetic (EM) and kinetic particle-in-cell code LSP to simulate the Z-pinch process. Later Schmidt *et al.* extended the applications of LSP code to fully kinetic simulations of dense plasma focus devices, which were designed to produce fusion neutron resources.[19,20] Recently, the LSP code was used to simulate and assess the ion kinetic effects in a laser direct-drive capsule implosion experiment.[21] All these researches mainly focused on the neutron yields and production mechanism, rather than on the microscopic mechanisms of Z-pinch and focus.

Two years ago, we realized the particle-in-cell simulation of the rarefied deuterium shell Z-pinch in China.[22] In principle, the profiles and evolution of magnetic field obtained in the PIC simulation are believed to have higher reliability. Therefore, due to the lack of measured profiles of magnetic field during the Z-pinch process, they could be approximately considered as the real magnetic field in the Z-pinch plasma. So we can understand the validity of MHD simulation of the Z-pinch plasma under very low mass density through comparing their evolvements obtained in the MHD and PIC simulations. At the same time the comparison can help us to in depth understand the Z-pinch mechanism in physics.

It is a crucial matter for Z-pinch radiation MHD simulation that the magnetic field evolution and the radiation emission and transport are accurately modeled because the used physical models and parameters for the magnetic field and radiation may largely affect the simulated results. When the mass density of simulated plasma is very low, the produced radiation is quite weak and can be neglected in the simulation. So we can focus on the magnetohydrodynamic behavior of the rarefied deuterium shell Z-pinch.

In this paper, we show the statistical results of mass density evolution in the PIC simulation of the rarefied deuterium shell Z-pinch in Subsection 2.1. The Z-pinch of the same shell will be simulated by our one-dimensional(1D) MHD code. How the electrical resistivity affects the magnetic field evolution and the dynamic process of Z-pinch is investigated by artificially modifying the resistivity. The results are presented in Subsection 2.2. The comparison between the PIC and MHD simulation results is carried out in Subsection 2.3 to explore the applicability of MHD simulation of Z-pinch under very low plasma density. Sections 3 and 4 are the discussion and conclusions, respectively.

2. Simulations of the rarefied deuterium plasma shell Z-pinch

The rarefied deuterium plasma shell Z-pinch, which was simulated by a particle-in-cell code,[22] is now simulated by our 1D radiation MHD code.[12,23] At the beginning, the inner radius $r_{\rm in}$ of the shell is 0.6 cm, the outer radius $r_{\rm out}$ is 1.0 cm, and its height is 1.0 cm. The mass per unit length of the plasma shell is 1.0×10^{-12} g/cm, and the matched current is taken as $I(t)=433\sin^4(\pi t/2T_0)$ A, where t is the time and T_0 is the rising time of the current (I) from 0 to peak. Here T_0 is assumed to be 50 ns. The mass density of the shell is about 4.97×10^{-13} g/cm^3. The emission of radiation would be very weak during the shell Z-pinch due to very low plasma density, and the radiation effect on the shell Z-pinch dynamic process would not be considered in its MHD simulation. The free path of particle collision is still substantially smaller than the size of the shell, and the fluid description may be suitable for its magnetohydrodynamic process. Therefore, we simulate the Z-pinch process of the rarefied deuterium plasma shell by the 1D MHD code. Generally, the Spitzer resistivity ($\eta=5.2\times10^{-3}z\ln\Lambda/T^{3/2}$ Ω·cm, where z is the ionization degree, $\ln\Lambda$ is the Coulomb logarithm, and T is the plasma temperature in units of eV) is adopted in solving the magnetic field equation. The resistivity is sometimes modified by being multiplied by a factor for obtaining better results. When a multiplier of 2 is applied to the Spitzer resistivity, which approximately means that the resistivity perpendicular to the azimuthal magnetic field is adopted in the simulation.

2.1. Mass density evolution in the PIC simulation

Figure 1 shows the mass density profiles obtained in the PIC simulation at some times in the Z-pinch process of the shell. In the first 45 ns of the pinch, we can find that the electrical particles seem to be attracted to the center (see Fig. 1(a)), and at the same time they are driven towards the inner surface of the shell and enter into the mass density profile evolution (see Fig. 1(b)). As a whole, the particle shell under the driven current firstly behaves as a snowplow-like implosion, but with some kinds of oscillation and instability development in the mass density profile. The instability has been restrained temporarily at the end of the snowplow-like implosion phase. Thereafter an intense shock wave is formed, and continues to move inwards and evolves. Before 45 ns of the Z-pinch, the inner surface is almost stable, and the outer plasma is ploughed up together to form a more and more intense shock wave. After 45 ns, the mass density evolution is similar to shock compression.

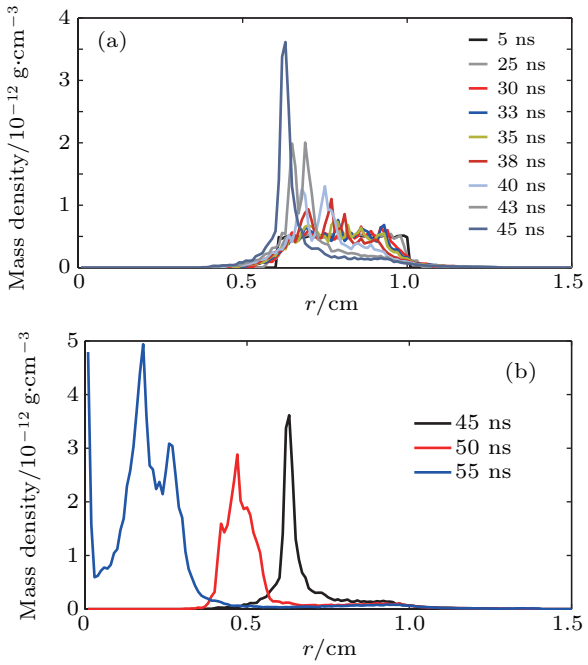


Fig. 1. (color online) Profiles of mass density (a) at 5 ns, 25 ns, 30 ns, 33 ns, 35 ns, 38 ns, 40 ns, 43 ns, and 45 ns, and (b) at 45 ns, 50 ns, and 55 ns, obtained in the PIC simulation of the shell.

2.2. Results of MHD simulation

In the Lagrangian MHD simulation, we can record the flow lines of the simulated mass points. Figure 2 shows the calculated streamlines of the same rarefied deuterium plasma shell Z-pinch. It shows the integrated characteristic of the Z-pinch process of the shell. The outermost mass point exhibits a little expansion outwards, and a few innermost mass points move inwards earlier obviously. The trajectories of movement of the mass points are very similar to our previous simulation results about Z-pinches.[23,24]

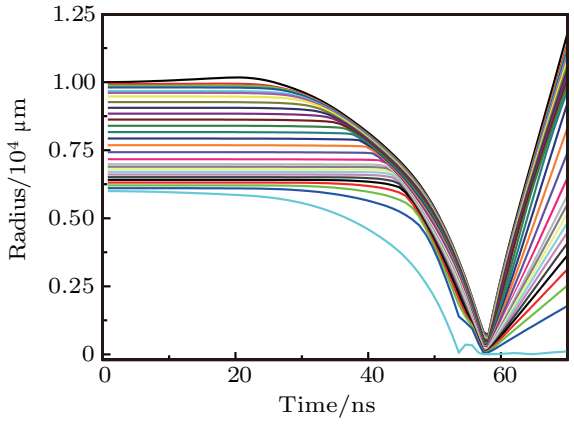


Fig. 2. (color online) Streamlines of the rarefied deuterium plasma shell Z-pinch, obtained in the MHD simulation, in which the used Spitzer resistivity is enlarged by being multiplied by a factor of 2.

Figure 3 shows the mass density evolutions of the shell with two different multipliers of resistivity. In the case of a multiplier of 2, a weak shock wave is generated early in the Z-pinch, and is gradually enhanced as time goes by (see Fig. 3(a)). Before 45 ns of the Z-pinch, the inner surface moves inwards a bit, and the outside plasma is ploughed up by a shock wave. After 45 ns the mass density evolution is roughly similar to that calculated by the PIC code (see Fig. 1(b)), where all evolve in the shock compression scheme. While the shock wave is gradually weakened (see Fig. 3(b) with the multiplier 1000) with the increase of used multiplier in Spitzer resistivity due to the enhanced magnetic diffusion, which increasingly cause the inward movement of the inner surface of the shell, and the expansion of the outer surface of the shell.

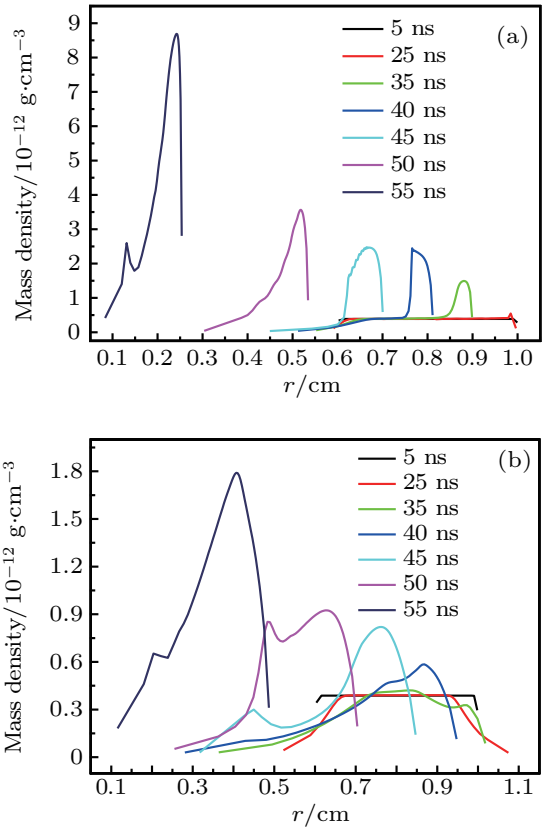


Fig. 3. (color online) Profiles of mass density at 5 ns, 25 ns, 35 ns, 40 ns, 45 ns, 50 ns, and 55 ns, calculated in MHD simulations with the used multipliers of (a) 2 and (b) 1000.

In Z-pinch MHD simulation it is well known that the simulated Z-pinch process is sensitive to the modification of plasma resistivity. Compared with the macroscopic experimental data, the good simulated results could be obtained through the resistivity modification, but the dynamic process presented in the simulation might be changed a lot, even deviated from the reasonable one. Now we begin to explore how the modified resistivity affects the magnetic field evolution and the dynamic process of Z-pinch in the MHD simulation.

Figure 4 shows the variations of magnetic field profiles with the Spitzer resistivity multiplier (such as 2, 50, 100, 500, and 1000) in MHD simulation. From Fig. 4 we can clearly see that the magnetic field in the inner part of the shell increases and the maximum field decreases (i.e., the profiles turn flat gradually) because of the enhancement of magnetic field diffusion.

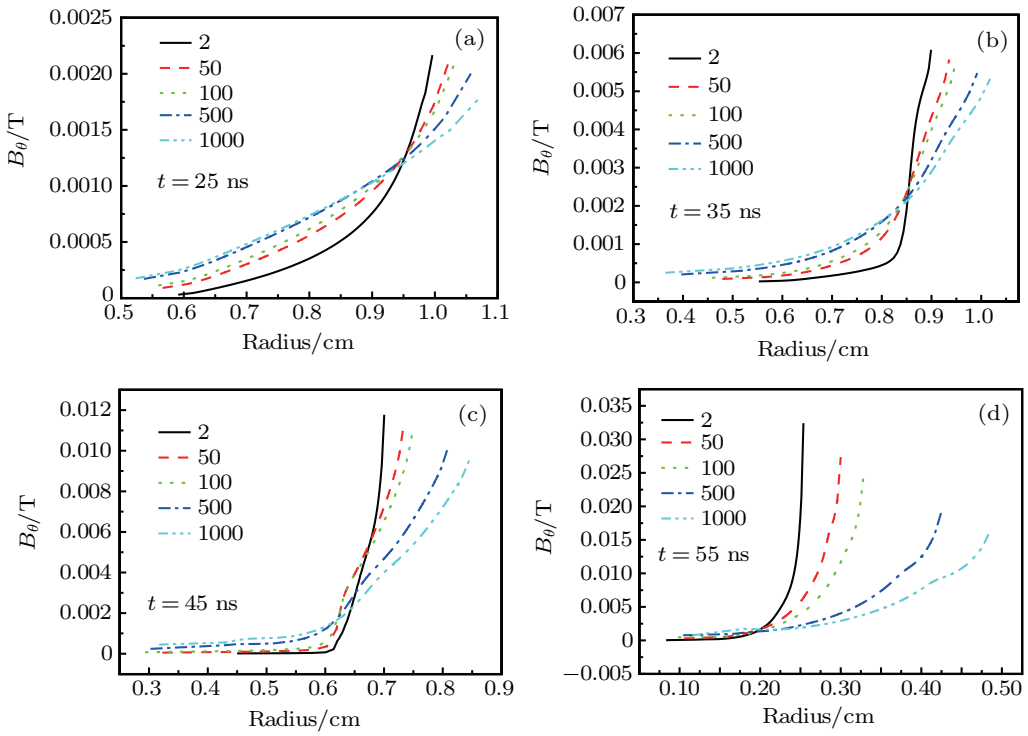


Fig. 4. (color online) Variations of magnetic field profile with the used multiplier in the MHD simulation at 25 ns (a), 35 ns (b), 45 ns (c), and 55 ns (d).

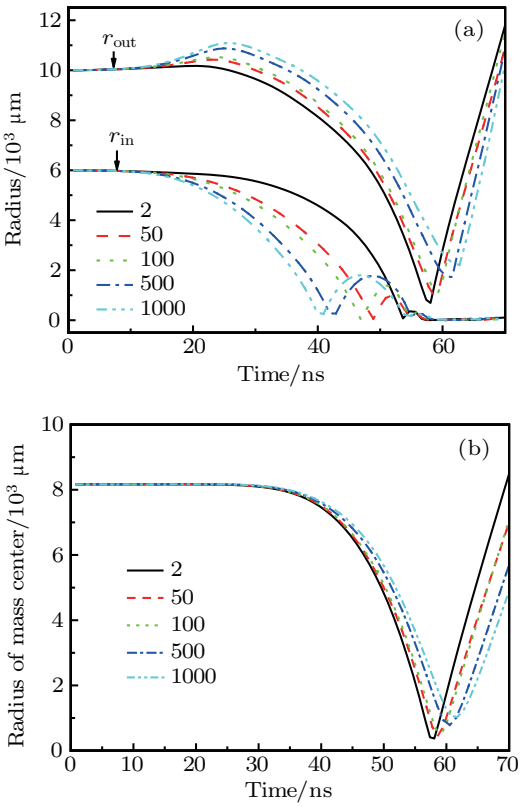


Fig. 5. (color online) Radius variations of outer and inner interfaces (a), and mass center (b) of the shell with time under a few multipliers applied to Spitzer resistivity in the MHD simulation.

Figure 5(a) shows the implosion characteristics of the outer and inner interface of the shell, and figure 5(b) displays the behaviors of the mass center during implosion. We can find that the plasma shell first expands outwards and inwards simultaneously (see Fig. 5(a)) at the early phase, and the expansion will turn more obvious with the multiplier increasing due to the enhanced thermal pressure and magnetic field diffusion. Whereas the mass center of the shell keeps stable at this phase (see Fig. 5(b)). With the increase of the resistivity, the Z-pinch process of the outer part of the shell is delayed and slows down gradually, and one of the inner part occurs earlier step by step. The latter even seems to pinch independently because it experiences an increasing Lorentz force induced by current and magnetic field diffusion into this area. So, using a too large multiplier can cause an unreasonable dynamic process of the Z-pinch. The implosion process of the mass center also delays with the multiplier increasing (see Fig. 5(b)).

Figure 6 presents the compression status of the shell with the increasing of resistivity. The convergence ratio is defined as the value of radius at time t, $r(t)$, divided by the value $r(0)$ at time $t = 0$, $r(0)$ at a certain place. Figures 6(a) and 6(b) show the behaviors of convergence ratios of the outer interface and the mass center, respectively. Basically, the latter can well express the compression behavior of the Z-pinch plasma, and is higher than the former. However, only the convergence ratio of the outer interface could be inferred from the experimental images, such as the streak image, x-ray image and laser shadow image of the Z-pinch plasma. All kinds of convergence ratios decrease with resistivity increasing.

Figure 7 exhibits how the mass density profiles evolve with the Spitzer resistivity multiplier in the MHD simulation

of the plasma shell. Figure 7(a) shows that the plasma shell expands, and the expansion becomes more severe with the increase of multiplier (just like that seen in Fig. 5(a)). At 25 ns an intense shock in density is developed at the outer interface of the shell for the case of multiplier 2. From 25 ns to 45 ns it develops more and more intensely by ploughing up more plasma into the shock. At 45 ns the shock also forms in the cases of the multipliers of 50 and 100 (see Fig. 7(c)). However, there is no shock forming in the cases of the multiplier of 500 and 1000 until 55 ns (see Fig. 7(d)). Therefore, the dynamic process of the Z-pinch changes very much if the resistivity used in the MHD simulation is artificially largely modified.

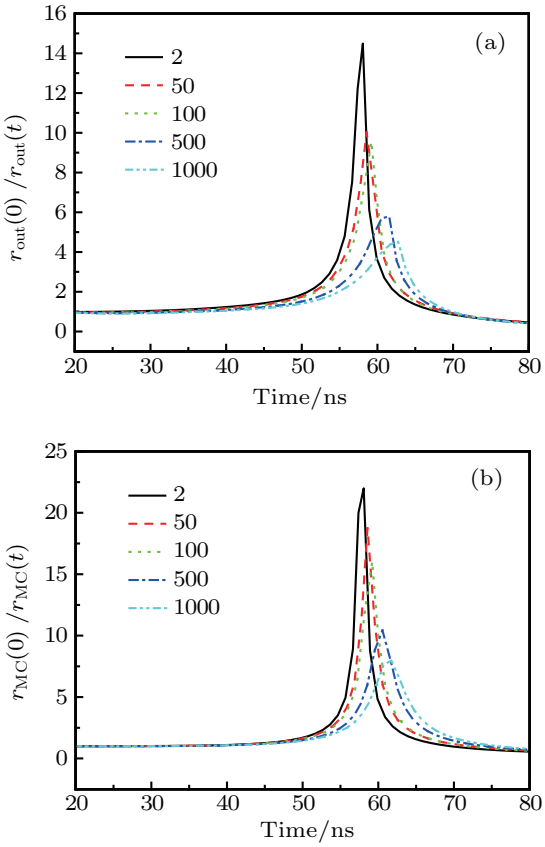


Fig. 6. (color online) Variations of convergence ratio of outer interface (a) and mass center (b) of the shell with time under a few multipliers used in the MHD simulations.

Figure 8 shows the variations of electron and ion temperatures in the middle of the shell in the Z-pinch process. We can clearly find that the peak electron temperature is about 1.5 keV, and it increases with the used multiplier, mainly the enhanced ohmic heating, and that it almost saturated at about 4 keV when the multiplier is larger than 100. While the peak ion temperature is about 5.5 keV in the case of multiplier 2, and it declines with the multiplier increasing mainly for the reduction of compression degree of the shell, i.e., the reduction of pdV work. It becomes about 0.5 keV in the case of multiplier 1000. We can also note that the widths of the pulses at half maximum temperature are about 2 ns∼6 ns as the multiplier increases from 2 to 1000. This increase implies that the compression degree of the plasma shell declines, and the implosion velocity declines too.

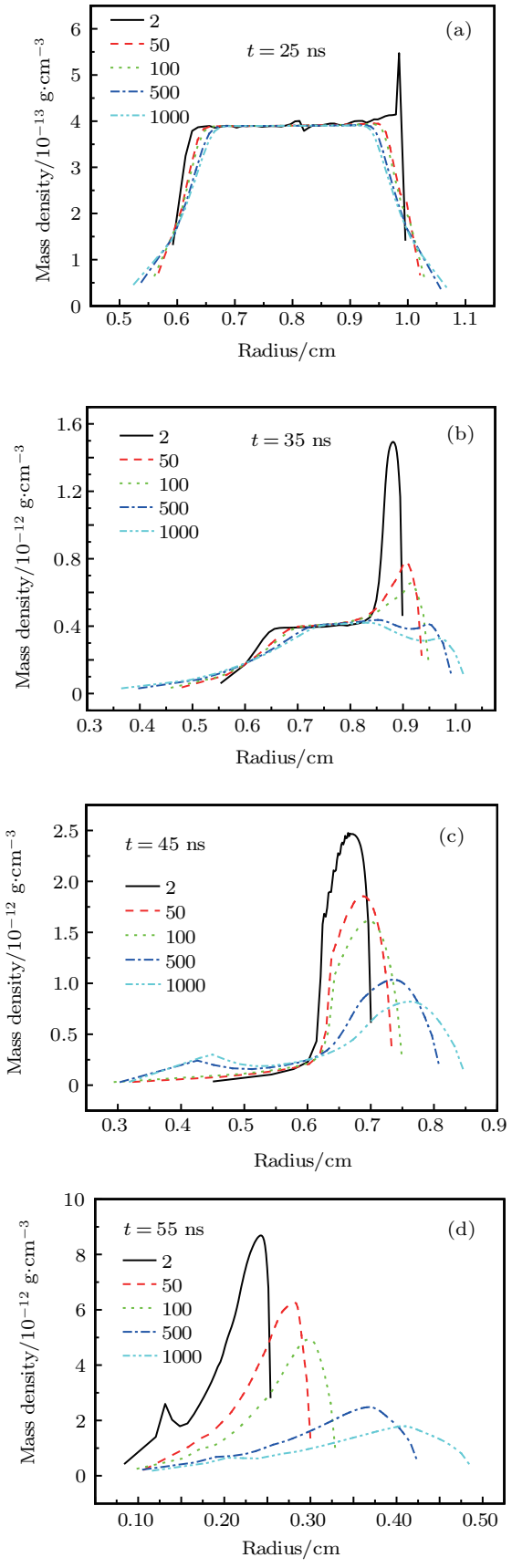


Fig. 7. (color online) Variations of mass density profiles with the used multiplier in the MHD simulation at 25 ns (a), 35 ns (b), 45 ns (c), and 55 ns (d).

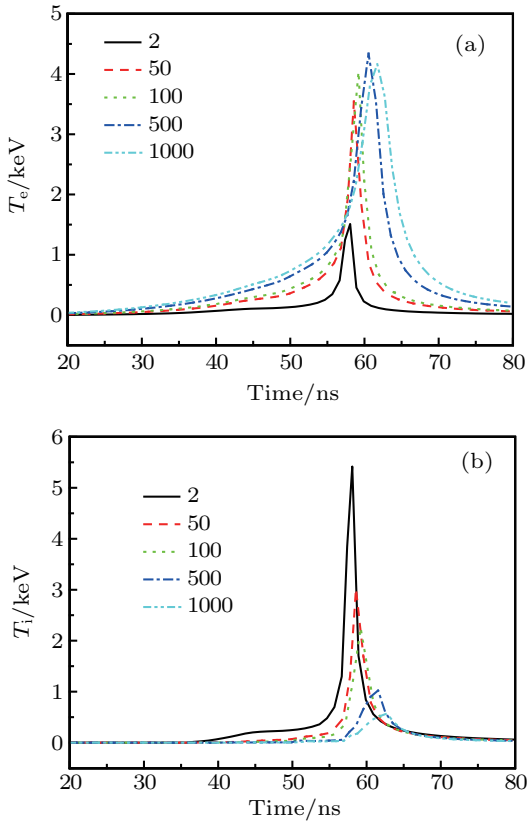


Fig. 8. (color online) Variations of electron (a) and ion (b) temperatures in the middle of the shell with time under a few multipliers used in the MHD simulations.

2.3. Comparison between the results of the PIC and MHD simulations

In the PIC simulation, a few millions of simulated particles are tracked, and the integrated evolution of the particle positions reveals the dynamic process of the shell Z-pinch.[22] For comparing the Z-pinch characteristics obtained by the MHD simulation with that by the PIC simulation, their mass center implosion trajectories are calculated. They are defined as $r_c = \int \rho r^2 \mathrm{d}r / \int \rho r \mathrm{d}r$ in the MHD simulation, and

$$r_c = \frac{\sum_i m_i^{\mathrm{ion}} r_i^{\mathrm{ion}}}{\sum_i m_i^{\mathrm{ion}}} = \frac{\sum_i r_i^{\mathrm{ion}}}{N_{\mathrm{ion}}}$$

in the PIC simulation, where the electron mass is neglected, m_i^{ion} is the ith deuterium ion mass, r_i^{ion} is the radius of the ith ion position, and N_{ion} is the total number of the deuterium ions. Figure 9 shows the result. The variations of the trajectory with the used multiplier are also plotted. From Fig. 9, it can be found that the trajectory calculated by the PIC simulation is very close to that by the MHD simulation before stagnation when a multiplier of 2 is used. However in the MHD simulation the Z-pinch plasma seems more compressible since a higher convergence ratio is achieved. Moreover, we can also find that the implosion in the PIC simulation is slightly faster than that in the MHD simulation from about 43 ns to 50 ns. After the stagnation the Z-pinch plasma moves outwards faster in the PIC simulation because at that time the electrons shortly move inversely to cause the current to quickly transfer to the outer area due to static repellency among electrons and their tiny mass. The exhibited differences in the two kinds of simulated Z-pinch processes reflect the differences in physical mechanism of Z-pinch. With the increasing multiplier the convergence ratio calculated by the MHD simulation declines, and it becomes almost the same as that calculated by the PIC simulation when a multiplier of 1000 is used. Although the two convergence ratios are the same, the implosion time turns longer, which implies that their dynamic processes are different.

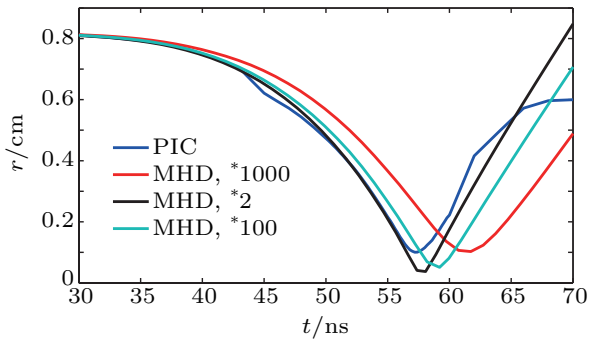


Fig. 9. (color online) Implosion trajectories of mass center of the plasma shell. The blue line represents the result obtained by the particle-in-cell simulation, while the other lines denote the results calculated by the MHD simulation, in which the used Spitzer resistivities are artificially enlarged by using multipliers of 2, 100, and 1000.

The magnetic field distribution and evolution are governed by the induction equation of magnetic field, which just includes the convection and diffusion terms due to adopting the Ohm's law

$$\boldsymbol{j} = \frac{1}{\eta}\left(\boldsymbol{E} + \frac{1}{c}\boldsymbol{u} \times \boldsymbol{B}\right),$$

where $\boldsymbol{j}$, $\boldsymbol{E}$, $\boldsymbol{B}$, η, and c are the current density, electric field, magnetic field, electric resistivity, and the light speed, respectively. The magnetic field flows with the plasma motion, and at the same time it diffuses into the plasma. For a given plasma shell, its Z-pinch dynamic process is mostly determined by the distribution and evolution of the magnetic field in it. The magnetic field convection depends on the plasma velocity, while its diffusion depends on the electric resistivity of plasma greatly. Unfortunately, so far there is no accurate expression of the electric resistivity for dense magnetized plasma, such as Z-pinch plasma. So for achieving better agreement of the simulated Z-pinch results with the experimental data, such as the convergence ratio, x-ray power and energy, the electric resistivity is required to be artificially modified more or less.[12,14] To what extent the Spitzer resistivity should be modified (i.e., how large the multiplier used in simulation should be) depends on the driven current level, and the material and configuration of load, as well as the used physical model and possibly the spatial dimension. The better simulated characteristic results

might be obtained through the modification, but the magnetic field evolution and detailed pinch process could be changed correspondingly. It is interesting and important to explore the variations of the magnetic field evolution and the dynamic process with the modification, and to compare the MHD simulation results with the PIC's under the lack of experimental data about the magnetic field evolution and microscopic dynamic process of Z-pinch.

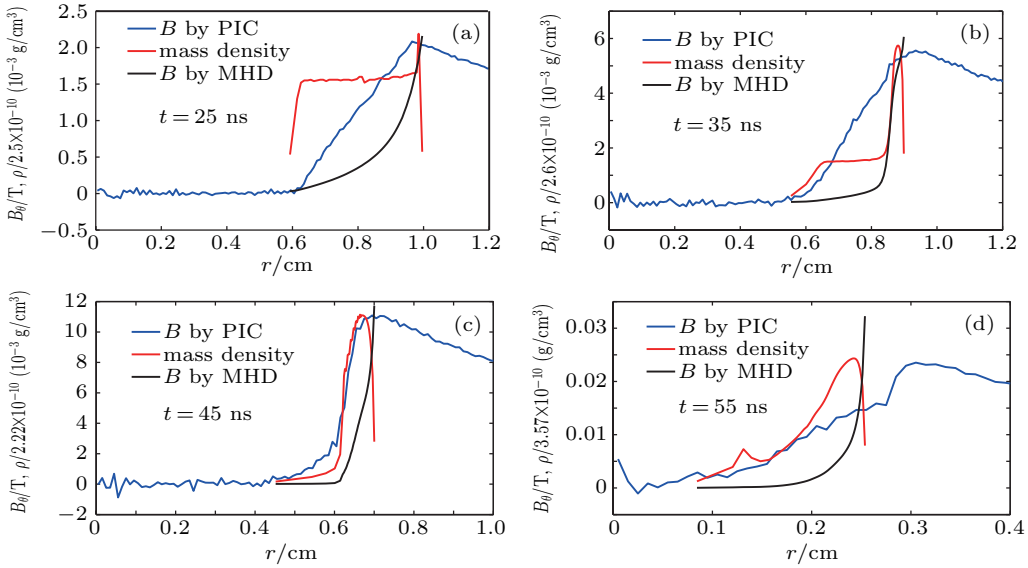


Fig. 10. (color online) Profiles of magnetic field and mass density at 25 ns (a), 35 ns (b), 45 ns (c), and 55 ns (d). The blue lines denote the magnetic fields from the simulation by using the PIC code, and the black lines represent the magnetic fields simulated by using the MHD code where the Spitzer resistivity is doubled. The red lines represent the mass density profiles simulated by the MHD code, and they are also used to mark the positions of the plasma shell.

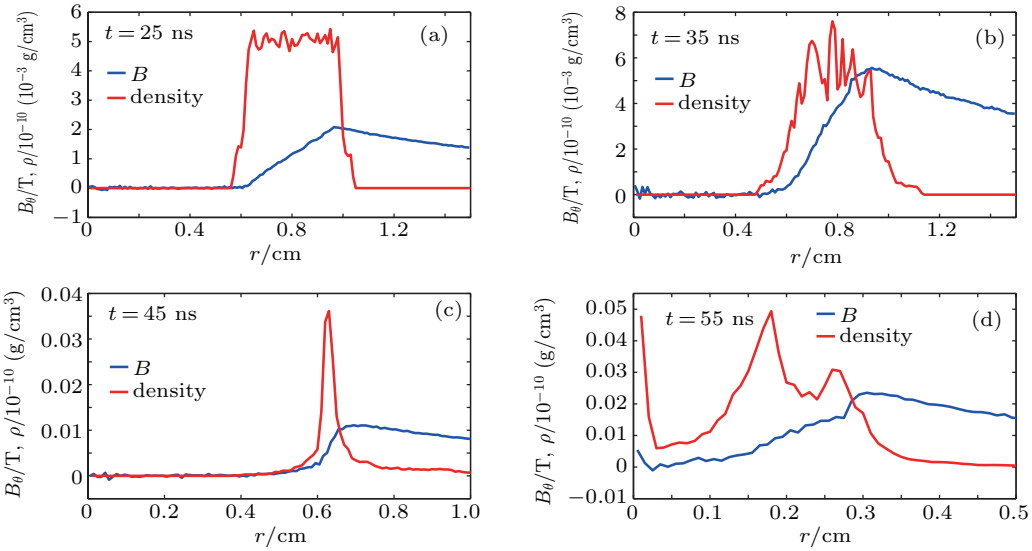


Fig. 11. (color online) Profiles of magnetic field and mass density obtained in the PIC simulation at (a) 25 ns, (b) 35 ns, (c) 45 ns, and (d) 55 ns. The blue lines denote the magnetic field, and the red lines the mass density profiles.

Here we compare the magnetic field profiles calculated by the MHD and PIC simulations at different times. Firstly figure 10 shows the profiles of magnetic field and mass density along the radius at four times in the case that the multiplier of 2 is applied to enlarge the Spitzer resistivity. It can be found that the magnetic field calculated by the MHD simulation is mainly distributed in the outer layer of the shell, and that the maximum field always presents itself in the outer surface of the shell. However, the magnetic field obtained in the PIC simulation diffuses into the whole shell, and at 55 ns the location of the maximum field moves behind from the place of the maximum field calculated by the MHD simulation obviously. So in the MHD simulation the shell Z-pinch is much like the magnetic piston implosion, and its convergence ratio can become higher. From Fig. 11 of the PIC simulated results we can find that the places of the maximum fields lag behind the places of the maximum mass density after 35 ns. That is to say, in the PIC simulation the magnetic field diffusion is relatively strong, and the field diffuses into the whole shell in the pinch process. Basically, the profile and evolution calculated in the

PIC simulation could be considered to have higher fidelity, which implies that the diffusion of the magnetic field is underestimated in this MHD simulation. Therefore, the Spitzed resistivity used in the MHD simulation of Z-pinch seems to require to be enlarged to a reasonable extent in order to enhance the diffusion.

When the used Spitzed resistivity is enlarged, the magnetic field diffusion will be enhanced and the convergence ratio becomes close to that obtained in the PIC simulation. Will their magnetic field profiles and evolutions become the same? Figure 12 shows the magnetic field profiles at four times, calculated by the MHD simulation, in which a multiplier 1000 is used to reduce the convergence ratio to a value close to that reached in the PIC simulation. Comparing them with the results presented in Fig. 10, it can be seen that the magnetic field diffusion into the shell is enhanced obviously, and that the position of the maximum magnetic field lags behind largely, i.e., the Z-pinch process slows down. While the magnetic field profiles are still quite different from the PIC's results, even though their convergence ratios are almost the same, which possibly implies that the used inductance equation of $\boldsymbol{B}$ could not accurately describe the magnetic field evolution in this very low density plasma.

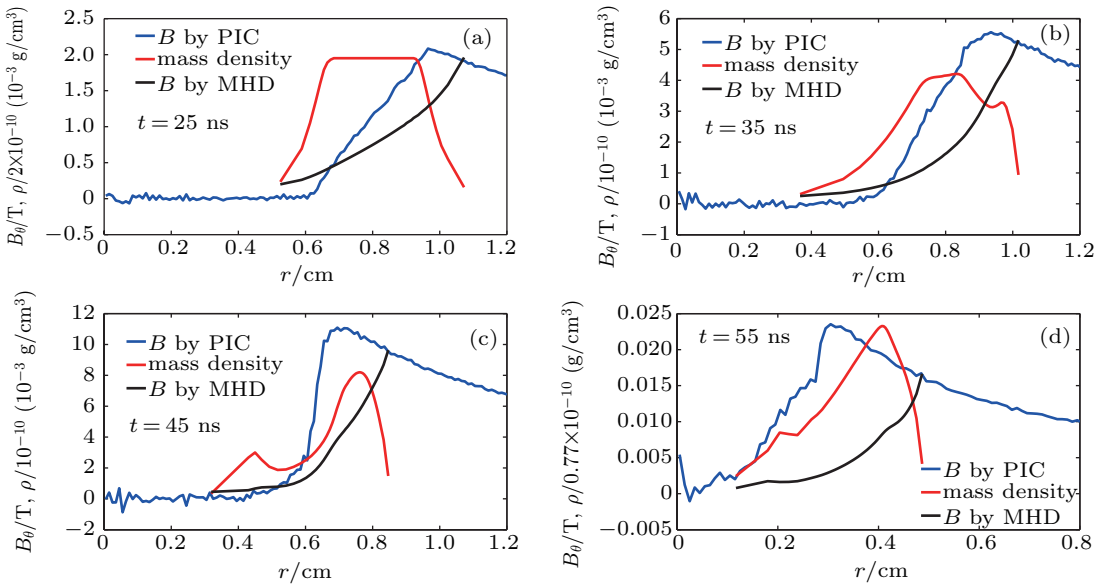


Fig. 12. (color online) Profiles of magnetic field and mass density at (a) 25 ns, (b) 35 ns, (c) 45 ns, and (d) 55 ns. The blue lines denote the magnetic field simulated by the PIC code, and the black lines represent the magnetic fields simulated by the MHD code where 1000 times the Spitzer resistivity is used. The red linesrefer to the mass density profiles simulated by the MHD code, and are also used to mark the place of the plasma shell.

3. Discussion

3.1. Mechanisms of Z-pinch under hydrodynamic and kinetic descriptions

In the MHD simulation of Z-pinch, the whole plasma shell is driven inwards by Lorentz force $\boldsymbol{j} \times \boldsymbol{B}$, and it keeps electrical neutralization as a whole. The mass density evolution depends on the fluid flow which is driven by the thermal pressure and Lorentz force exerted on the neutral electrically conductive fluid. However, in the PIC simulation of the Z-pinch, the mass density evolution depends on the movement of ions, which are governed by their experienced electric and magnetic forces (of course, and by the particle collisions if the collisions are included in the simulation). So, we might speculate that there would possibly exist the significant differences between the mass density distributions simulated by the particle-in-cell and magnetohydrodynamics codes. Figure 13 shows the electric and magnetic forces exerted on the ion in the radial direction in the plasma shell. They reveal that in the radial direction the forces exerted on the ion are mainly the electric force, which is several orders of magnitude larger than the magnetic force, and actually the electrostatic force produced by the charge separation between the ion and electron. From Fig. 13 we can find that at a certain time the direction of electric force along radius changes with position r, especially in the early phase it changes more considerably, for example, before 30 ns (see Figs. 13(a) and 13(b)). At a certain position it also changes from time to time. So the movement states of the ions are changeful and complicated. However, the direction of Lorentz force in the MHD simulation keeps unchanged all the time, pointing to the axis. That would cause the differences in the mass density evolution from the MHD simulation, especially in the early phase of the shell Z-pinch (see Figs. 1 and 3 and their comparison). Moreover it could be expected that there would exist instability development in a plasma shell Z-pinch even if the shell is totally uniform due to the electromagnetic interaction among the charged particles and field, which reflects the complexity of particle-charged flow to some extent.

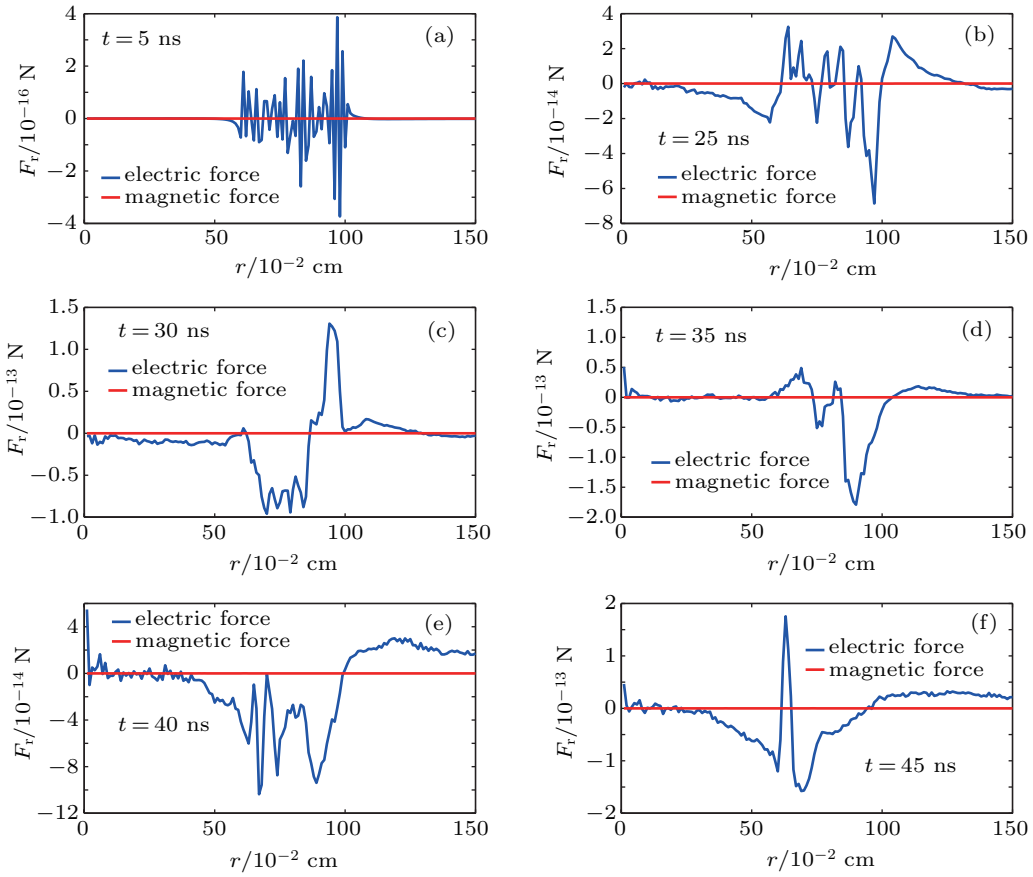


Fig. 13. (color online) Profiles of the electric (blue lines) and magnetic (red lines) forces exerted on ions in radial direction at (a) 5 ns, (b) 25 ns, (c) 30 ns, (d) 35 ns, (e) 40 ns, and (f) 45 ns. They are obtained in PIC simulation of the shell Z-pinch.

In the radial direction the electric and magnetic forces exerted on the electrons are comparable in magnitude,[22] while the forces exerted on the ions are mainly the electric forces. So, in the Z-pinch process the electrons should be first accelerated in axial electrical field and reach higher velocities, then they are driven inwards to the axis at the same time by the radial magnetic forces (i.e., Lorentz forces $-q\upsilon_z B_\theta$, where q and υ_z are the charge and the axial velocity of electron, respectively, and B_θ is the azimuthal magnetic field), which causes the separations between the electrons and ions because the ion mass is much larger than the electron's, and in turn a strong electrostatic field is produced. The produced electrostatic field attracts the ions to move towards the electrons. That is to say, the Z-pinch mechanisms are different under the descriptions of single fluid MHD and particle kinetics.

3.2. Applicability of MHD simulation

We cheerfully note that the mass density evolutions obtained in the PIC and MHD simulations are similar in the phase of shock wave compression after 45 ns (see Figs. 1(b) and 3(a)). The MHD simulation of the shell yields the qualitatively reasonable results, such as the profiles of density and magnetic field, and their variations with the resistivity modification. That is to say, the Z-pinch of a very low density plasma shell can still be simulated approximately by the magnetohydrodynamics, especially in its fast implosion phase.

However, compared with the magnetic field profile obtained in the PIC simulation, the diffusion of the magnetic field seems to be underestimated in the MHD simulation. Even though their convergence ratios become almost the same, the magnetic field in the PIC simulation distributed inside the shell is higher than that in the MHD simulation mostly. Theoretical analysis demonstrates that the ion inertial length ($c/2\pi f_{\rm pi}$, where $f_{\rm pi}$ is the ion plasma frequency) is comparable to the size of the shell with very low density considered in this paper. In this case, the magnetic field becomes mainly frozen into the electron fluid rather than the bulk plasma, and the two-fluid or Hall MHD model, even the PIC/fluid hybrid simulation would be used.[25–30] Therefore, in the wire-array Z-pinch (single-fluid) MHD simulation in which the processes of wire ablation and plasma expansion are considered, the plasma density needs to be truncated when it is too low.

When a radiation research of Z-pinch is located outside the Z-pinch plasma, such as the researches of radiation effect on material and the measurement of plasma opacity, the Z-pinch dynamic process will be relatively isolated from the interaction process of radiation and material. The requirement

for the accurate simulation of Z-pinch plasma might be relaxed to some extent, and a larger multiplier could possibly be used in resistivity modification to obtain a more reasonable x-ray radiation pulse waveform. While in the scheme of dynamic hohlraum for Z-pinch driven ICF the ablated implosion process of a capsule embedded in the dynamic hohlraum is tightly connected with the wire-array (liner) implosion process. The action process of the capsule depends on the implosion process of the plasmas outside the capsule. In this case, if a larger multiplier (say, several tens or hundreds) is used, the inner part or shell of the plasma profile will be driven to implode earlier due to the artificially enhanced magnetic diffusion, and in turn it will unexpectedly cause the capsule action earlier.

We should point out that the required multiplier to modify the resistivity nominally for more reasonable result of Z-pinch simulation would decline with the increase of atomic number due to the possibly high ionization degree for a certain current level. In this paper the largest multiplier 1000 is used to restrain the convergence ratio to a value close to the convergence ratio of the PIC simulation because the atomic number of deuterium is the smallest in all the elements.

4. Conclusions

The Z-pinch processes of the rarefied deuterium current-carrying shell are simulated by the MHD and PIC codes, respectively. Their results, especially the magnetic field and mass density profiles and evolutions, are analytically compared with each other. In the MHD simulation the variation trends of the implosion characteristic and mass density, magnetic field, convergence ratio and temperatures with the increasing resistivity are explored in detail. Firstly, compared with the magnetic field profiles obtained in the PIC simulation, the magnetic field diffusion cannot be adequately revealed in the MHD simulation under the very low plasma density, though the fluid dynamic behaviour is still qualitatively described. For accurately simulating the whole wire-array Z-pinch process, two-fluid or Hall MHD model, even the PIC/fluid hybrid simulation would be possibly required. Secondly, there is a significant difference in the evolution of mass density profile between the PIC and MHD simulations before 45 ns (during the snowplow like implosion phase) of the shell Z-pinch because of the different pictures of forces exerted on ions and fluid. After the shock formation in the PIC simulation, the mass density evolution is similar to that in the MHD simulation for the case of using multiplier 2 to some extent. Thirdly, the MHD simulation results suggest that the magnetic field diffusion is enhanced greatly by increasing the Spitzer resistivity used. In turn it causes the implosion characteristics to change from the shock compression to weak shock, even shockless evolution, and cause the shell to expand more obviously, thereby slowing down the implosion process and reducing the convergence ratio. The peak temperature of electron increases and then reaches a saturate value, while the peak temperature of ion declines with the increasing of resistivity used. Finally, in the MHD simulation, though the nominally better simulation results could be obtained by modifying the used resistivity, too large a multiplier is not suggested to be used in the Z-pinch in which the applied sample (object) is tightly coupled with the imploding plasma, such as the Z-pinch driven ICF in a dynamic hohlraum. If too large a multiplier is applied, it may induce the earlier inward movements of the inner plasma, and may generally result in an unreasonable implosion picture.

The particle-in-cell simulation of Z-pinch makes us understand in depth the microscopic kinetic process and the applicability of MHD simulation in very low plasma density. Practically, (radiation) MHD simulation is still the main numerical program tool in the physical understanding, experimental designs and data analysis of Z-pinch. In the future, the PIC simulation should be continuously developed and applied for the microscopic investigation of Z-pinch with higher mass density, and the physical models used in MHD simulation should be developed hand-running for the magnetic field evolution calculated accurately during the Z-pinch.

References

[1] Nash T J, Derzon M S, Chandler G A, *et al*. 1999 *Phys. Plasmas* **6** 2023

[2] Slutz S A, Douglas M R, Lash J S, Vesey R A, Chandler G A, Nash T J and Derzon M S 2001 *Phys. Plasmas* **8** 1673

[3] Bailey J E, Chandler G A, Slutz S A, Golovkin I, Lake P W, MacFarlane J J, Mancini R C, Burris-Mog T J, Cooper G, Leeper R J, Mehlhorn T A, Moore T C, Nash T J, Nielsen D S, Ruiz C L, Schroen D G and Varnum W A 2004 *Phys. Rev. Lett.* **92** 085002

[4] Slutz S A, Peterson K J, Vesey R A, Lemke R W, Bailey J E, Varnum W, Ruiz C L, Cooper G W, Chandler G A, Rochau G A and Mehlhorn T A 2006 *Phys. Plasmas* **13** 102701

[5] Jiang S Q, Ning J M, Chen F X, Ye F, Xue F B, Li L B, Yang J L, Chen J C, Zhou L, Qin Y, Li Z H, Xu R K and Xu Z P 2013 *Acta Phys. Sin.* **62** 155203 (in Chinese)

[6] Stygar W A, Awe T J, Bailey J E, *et al*. 2015 *Phys. Rev. ST Accel. Beams* **18** 110401

[7] Sanford W L 2008 *IEEE Trans. Plasma Sci.* **36** 22

[8] Lebedev S V, Beg F N, Bland S N, Chittenden J P, Dangor A E, Haines M G, Kwek K H, Pikuz S A and Shelkovenko T A 2001 *Phys. Plasmas* **8** 3734

[9] Lebedev S V, Beg F N, Bland S N, Chittenden J P, Dangor A E, Haines M G, Pikuz S A and Shelkovenko T A 2000 *Phys. Rev. Lett.* **85** 98

[10] Grabovskii E V, Mitrofanov K N, Oleinik G M and Porofeev I Yu 2004 *Plasma Phys. Rep.* **30** 121

[11] Wu J, Li X W, Li M, Li Y and Qiu A C 2017 *J. Phys. D: Appl. Phys.* **50** No. 40

[12] Ning C, Sun S K, Xiao D L, Zhang Y, Ding N, Huang J, Xue C and Shu X J 2010 *Phys. Plasmas* **17** 062703

[13] Chittenden J P, Lebedev S V, Bland S N, Ruiz-Camacho J, Beg F N and Haines M G 2001 *Laser and Particle Beams* **19** 323
[14] Thornhill J W, Whitney K G, Deeney C and LePell P D 1994 *Phys. Plasmas* **1** 321
[15] Birdsall C L and Langdon A B 1991 *Plasma Physics Via Computer Simulation* (New York: Adam Hilger)
[16] Welch D R, Rose D V, Clark R E, Mostrom C B, Stygar W A and Leeper R J 2009 *Phys. Rev. Lett.* **103** 255002
[17] Welch D R, Rose D V, Thoma C, Clark R E, Mostrom C B, Stygar W A and Leeper R J 2010 *Phys. Plasmas* **17** 072702
[18] Welch D R, Rose D V, Thoma C, Clark R E, Mostrom C B, Stygar W A and Leeper R J 2011 *Phys. Plasmas* **18** 056303
[19] Schmidt A, Tang V and Welch D 2012 *Phys. Rev. Lett.* **109** 205003
[20] Schmidt A, Link A, Welch D, Meehan B T, Tang V, Halvorson C, May M and Hagen E C 2014 *Phys. Plasmas* **21** 102703
[21] Le A, Kwan T J T, Schmitt M J, Herrmann H W and Batha S H 2016 *Phys. Plasmas* **23** 102705
[22] Ning C, Feng Z X, Xue C and Li B W 2015 *Phys. Plasmas* **22** 022710
[23] Ning C, Yang Z H and Ding N 2003 *Acta Phys. Sin.* **52** 415 (in Chinese)
[24] Ning C, Ding N, Liu Q, Yang Z H, Fan W B and Zang Y 2006 *Chin. Phys. Lett.* **23** 1857
[25] Martine M Y 2010 "Generalized Ohm's Law at the Plasma-Vacuum Interface", Ph. D. Dissertation (America: Cornell University)
[26] Srinivasan B and Shumlak U 2011 *Phys. Plasmas* **18** 092113
[27] Gyergyek T and Kovacic J 2015 *Phys. Plasmas* **22** 093511
[28] Sgro A G and Nielson C W 1976 *Phys. Fluids* **19** 126
[29] Fruchtman A 1991 *Phys. Fluids B* **3** 1908
[30] Huba J D 1995 *Phys. Plasmas* **2** 2504